Carbohydrate Polymers 111 (2014) 433–441

Contents lists available at ScienceDirect

Carbohydrate Polymers

journal homepage: www.elsevier.com/locate/carbpol

Decanoic acid grafted oligochitosan nanoparticles as a carrier for insulin transport in the gastrointestinal tract

Xuli Du[a], Jian Zhang[a], Yan Zhang[b], Shuang Li[a], Xia Lin[c], Xing Tang[a], Yu Zhang[a], Yanjiao Wang[a,*]

[a] Department of Pharmaceutics, Shenyang Pharmaceutical University, Wen Hua Road No. 103, Shenyang 110016, China
[b] Normal College, Shenyang University, Shenyang 110044, China
[c] School of Pharmacy, Shanghai Jiao Tong University, Shanghai, China

ARTICLE INFO

Article history:
Received 20 February 2014
Received in revised form 11 April 2014
Accepted 11 April 2014
Available online 21 April 2014

Keywords:
Oligochitosan
Decanoic acid
Insulin nanoparticles
Ionic crosslink
Antidiabetic

ABSTRACT

The objective was to explore the potential of decanoic acid grafted oligochitosan nanoparticles (CSO-DA NPs) as a carrier for insulin. The insulin-loaded CSO-DA NPs obtained by varying the pH and concentrations of CSO and DA had a particle size of 200.6 ± 71.2 nm, with an entrapment efficiency and loading efficiency of 61.18% and 5.56%, respectively. An in vitro study of the formulation showed typical burst of insulin and pH-dependent characteristics. The NPs administered by the in situ loop method were effective in lowering the serum glucose level of rats which was based on the synergistic effect of adhesion of CSO and permeation enhancing effect of DA. In particular, the 50 IU/kg-dose of CSO-DA NPs reduced the serum glucose level by 57.18%. Histopathology investigations showed that the CSO-DA NPs had a low toxicity. Therefore, CSO-DA nanoparticles appear to be promising vehicles for insulin transport through the intestinal mucosa.

1. Introduction

Insulin is usually administered by subcutaneous injection in clinical situations but, ideally, the oral route is by far the most convenient and comfortable way of delivering insulin. However, oral administration of pure insulin solution is totally ineffective in reducing blood glucose levels. It is due to the intrinsically poorly absorbable characteristic through the intestinal membrane and the highly susceptible characteristic to enzymatic degradation in the gastrointestinal (GI) tract. Entrapment of peptide drugs in nanocarriers protects them against the harsh environment of the GI tract until they are absorbed or released in intact particulate form (Makhlof, Tozuka, & Takeuchi, 2011). This leads to the rising needs to develop new formulation strategies emphasizing on the assembly of insulin and excipients into a physical structure to maintain the stability and increase the bioavailability of insulin. In recent decades, numerous attempts have been made to deliver drugs across the intestinal mucosa, such as using mucoadhesives (Zhang et al., 2012), pH-sensitive methods (Nguyen et al., 2011), chemical modification (Asada et al., 1995), anti-proteases (Aoki, Morishita, & Takayama, 2005) and different formulations and dosage forms (Fetih et al., 2006; Tozaki et al., 1997). In these approaches, absorption enhancers, including surfactants, bile salts, chelating agents and fatty acids, are one of the most promising methods.

In recent years, sodium decanoate, the sodium salt of the aliphatic saturated 10-carbon medium chain fatty acid decanoic acid (DA), has been shown to promote the transmucosal absorption of drugs, apparently by enhancing the permeability of the paracellular pathway (Chao et al., 1999). It is reported that decanoate induces in intestinal epithelial monolayers a fast and reversible reduction in transepithelial resistance (TER), which is based on a change in tight junctions, while the transcellular (cell membrane) resistance remains unaffected (Krug et al., 2013). Also, the kinetics and reversibility of the mechanism indicate that sodium decanoate is a promising candidate for the development of intestinal delivery strategies for drugs. Furthermore, decanoic acid is present in dairy products, particularly milk and it is approved by the FDA as a direct food additive for human consumption.

Chitosan, the cationic (1-4)-2-amino-2-deoxy-β-D-glucan produced from chitin (Muzzarelli, 2010; Muzzarelli et al., 2012) is being studied extensively in several sophisticated fields such as immunochemistry, medical aids, enzyme immobilization and membrane technology (Muzzarelli, 1983; Muzzarelli et al., 2012) owing to its biocompatibility, biodegradability, and absence of

* Corresponding author. Tel.: +86 024 23986343; fax: +86 024 23911736.
E-mail address: tanglab@126.com (Y. Wang).

http://dx.doi.org/10.1016/j.carbpol.2014.04.048
0144-8617/

toxicity. It is a mucoadhesive and sorbefacient polysaccharide, which can adhere to the surface of epithelial cell membrane through ionic interactions (Lehr, Bouwstra, Schacht, & Junginger, 1992) and reduce transepithelial electrical resistance and then transiently open tight junctions between epithelial cells to enhance insulin absorption (Artursson, Lindmark, Davis, & Illum, 1994; Illum, 1998). Chitosan has also been employed as a pharmaceutical excipient in oral drug formulations in order to improve the dissolution of poorly absorbable drugs (Imai, Shiraishi, Saitô, & Otagiri, 1991; Sawayanagi, Nambu, & Nagai, 1982a, 1982b) or for sustained release of drugs by a process of slow erosion from a hydrated compressed matrix (Miyazaki, Ishii, & Nadai, 1981; Miyazaki, Yamaguchi, Yokouchi, Takada, & Hou, 1988; Takayama et al., 1990). In the recent decades, chitosan can be used in solutions, hydrogels and nano/microparticles, while an endless array of chitosan derivatives with customized biochemical properties can be prepared through facile conjugation of side chain moieties to solvent-accessible amine and hydroxyl groups (Smith, Ravindranathan, Jayanthi, Suresh Kumar, & Zaharoff, 2014). PEG-grafting (Makuška & Gorochovceva, 2006), sulfonation (Qiao et al., 2011), quaternarization (Mao et al., 2001) and carboxymethylation (Gu, Song, Li, & Sui, 2011) are the common methods to modify chitosan. Oligochitosan (CSO) is a natural degradation product of chitosan. It is soluble in water and preserves the beneficial properties of chitosan. In addition, CSO has reactive amino and hydroxyl groups, and so many CSO derivatives for pharmaceutical application can be obtained by chemically altering its properties under mild reaction conditions (Kim et al., 2005; Kwon et al., 2003; Yoksan, Matsusaki, Akashi, & Chirachanchai, 2004). To sum up, CSO is regarded as an ideal carrier for insulin delivery. In consideration of the dual mechanism of CSO and DA, a novel material was synthesized which combined both of their properties to enhance the oral effect of insulin.

The aim of this work was to explore the potential of decanoic acid grafted oligochitosan nanoparticles (CSO-DA NPs) as a carrier for delivering insulin by the oral route. The formulations of insulin-loaded NPs made of CSO-DA and CSO were designed and characterized including the particles size distribution, morphology, insulin loading and in vitro release. The biological efficacy after ileum administration of NPs in normal rats was studied.

2. Materials and methods

2.1. Materials

Porcine insulin (27.5 IU/mg) was purchased from Xuzhou Wanbang Biochemical Pharmaceutical Co., Ltd., (China). Oligochitosan (CSO, Mw = 5 kDa, with a 90% degree of deacetylation) was from Zhejiang Goledn-Shell Pharmaceutical Co., Ltd., (China). Decanoic acid (DA) and 2, 4, 6-Trinitrobenzenesulfonic acid solution (TNBS) was from Aladdin Chemistry Co., Ltd (Shanghai, China). 1-Ethyl-3-(3-dimethylaminopropyl) carbodiimide hydrochloride (EDC) was purchased from Sigma (St. Louis, MO, USA) and sodium pentobarbital was obtained from Chengdu Grecia Chemical Technology Co., Ltd (Shandong, China).

SD rats (200 ± 20 g) were purchased from the Experimental Animal Center of Shenyang Pharmaceutical University and treated, during the entire study, according to protocols evaluated and approved by the University Ethical Committee.

2.2. Synthesis of CSO-DA

2.2.1. Preparation of CSO-DA

The complex reaction to prepare oligochitosan-decanoic acid (CSO-DA) took place between the carboxyl groups of DA and the amine groups of CSO in the presence of EDC (Hu, Wu, Du, You, & Yuan, 2008; Zhao et al., 2012). Firstly, CSO (0.5 g) was dissolved in 30 ml deionized water (DI water), and decanoic acid was dissolved in 20 ml methanol. They were then heated to 80 °C under stirring. The CSO solution was added to the mixture after EDC was mixed into the DA solution, and the coupling reaction was carried out at 80 °C for 5 h. Then, the reaction solution was cooled to room temperature and dialyzed against distilled water using a dialysis membrane (Mw: 3.5 kDa) for 24 h to remove water-soluble byproducts and then the dialyzed product was lyophilized. Finally, the lyophilized product was washed three times with 20 ml ethanol to remove unreacted DA. The suspension was then passed through a 0.8 μm millipore filter and the precipitate was collected, and dried to obtain the DA-grafted-CSO copolymer (CSO-DA).

2.2.2. Determination of the degree of substitution of CSO-DA

The substitution degree (SD%) of amino groups was measured by the TNBS method (Bernkop-Schnürch & Krajicek, 1998), using a calibration curve obtained by the amino-group determination of a series of CSO solutions with different concentrations. Then 10.00 mg CSO-DA was suspended in 10 ml distilled water and incubated with 2 ml 4% $NaHCO_3$ and 2 ml 0.1% TNBS at 37 °C for 2 h. Subsequently, 2 ml 2 N HCl solution was added to the mixture to neutralize the residual of $NaHCO_3$. The final reaction product was measured by UV spectroscopy at an absorbance wavelength of 344 nm.

An ^1H NMR spectrum was obtained to confirm the synthesis of CSO-DA. The sample was measured at 25 °C with about 0.05 wt.% D_2O solution using an NMR spectrometer.

IR spectra of resulted products were measured by EQUINOX 55-type spectrometer (Bruker Co., Germany) to determine the chemical interaction between CSO and DA.

2.3. Investigation of the conditions for the formulation of NPs

2.3.1. Preparation of CSO NPs

CSO-NPs were prepared by the ionotropic gelation between CSO with TPP according to the process reported by Calvo, Vila-Jato, and Alonso (1997). CSO and TPP were respectively dissolved in deionized water at different concentrations. Then, different volumes of TPP solutions were added dropwise to CSO solutions at different pH values and the different concentrations were passed through a syringe needle under magnetic stirring at 25 °C. The particle size and colloidal stability of the products were used to select the best formulation parameters to prepare the nanoparticles.

2.3.2. Preparation of CSO-DA NPs

CSO-DA NPs were prepared according to the procedure previously developed by our group. CSO-DA was dissolved in deionized water at a concentration of 1.0 mg/ml and the pH was adjusted to 5.5. Then, 1.0 ml TPP solution was added drop-wise to 10.0 ml CSO-DA solution using a magnetic stirrer. The suspension obtained was stirred for a further 30 min.

For the association of insulin to CSO-DA NPs, insulin was premixed in TPP solution. The concentration of insulin ranged from 0.5 mg/ml to 1.5 mg/ml, and nanoparticles were obtained.

To avoid particle aggregation, the suspensions were mixed with an equal volume of 1% trehalose (pH 6.0) which served as a cryoprotectant. The NPs were then lyophilized and stored at 4 °C until required for further studies.

2.3.3. In vitro characterization

The particle size was determined by dynamic light-scattering using a Nicomp380/ZLS apparatus (Santa Barbara, CA). Zeta potential determinations were made by the laser doppler electrophoresis (LDE) method using the same instrument.

The morphology of the particles was examined under transmission electron microscopy (TEM) and scanning electron microscopy (SEM) provided by the China Medical University and Institute of Metal Research, Chinese Academy of Sciences, respectively. A drop of NPs suspension was added to a carbon-coated copper grid and stained with osmium tetroxide. After drying completely, the TEM analysis was carried out. A small sample of the freeze-dried powder was placed on a conductive tape and uniformly sprayed with gold. Then, the shape of the NPs was examined using SEM images.

The entrapment efficiency (EE%) and loading efficiency (LE%) of insulin in NPs were measured after centrifugation of the NP suspensions (40,000 × rpm, 4 °C for 2 h, Hitachi koki Co., Ltd. Japan) and the amount of drug in the supernatant was assayed using HPLC. The HPLC system consisted of an isocratic pump (Hitachi L-7420, Japan), a UV–vis detector (Hitachi L-7100, Japan), and a Phenomenex® Prodigy 5u ODS3 100A column (250 mm × 4.60 mm, Phenomenex., USA). The mobile phase consisted of 0.2 M sulfate buffer solution, to which 2 ml phosphoric acid was added, and the pH of the solution was adjusted to 2.3 by ethanolamine (A) and acetonitrile (B) (A:B = 73:27, v/v), and the flow rate was 1.0 ml/min. The detection wavelength was 214 nm and the column temperature was maintained at 25 °C.

The drug entrapment efficiency (EE%) and loading efficiency (LE%) were calculated according to the following equations:

$$\text{EE\%} = \frac{\text{total drug} - \text{drug in supernatant}}{\text{total drug}} \times 100 \quad (1)$$

$$\text{LE\%} = \frac{\text{total drug} - \text{drug in supernatant}}{\text{weight of nanoparticles}} \times 100 \quad (2)$$

2.4. In vitro release of insulin nanoparticles

Insulin released from the freeze-dried NPs was determined by incubating nanoparticles at 37 °C in phosphate buffer (pH = 1.2, 7.4) with mild stirring. Ten mg samples of nanoparticles were redissolved in 5 ml buffer and at pre-determined time intervals (0.5, 1, 2, 4, 6 h), samples were centrifuged (40,000 × rpm, 30 min), and the supernatant was removed and replaced by fresh buffer. The amount of free insulin was determined by HPLC. The amount of insulin released was expressed as a percentage of the total insulin associated with the NPs as calculated from the loading efficiency.

2.5. Bioactivity stability

In order to determine the bioactivity of the nanoparticles, the lyophilized nanoparticles redissolved in normal saline were subcutaneously injected into normal rats at a dose of 5 IU/kg. Insulin solution in normal saline (5 IU/kg) served as a control. Before and after administration, the hourly blood glucose levels were measured by a glucometer (ACCU-CHEK® Active Sensor, Roche Diagnostics, Mannheim, Germany).

2.6. Absorption experiments using the in situ loop method

Intestinal absorption was evaluated by the methods described previously with slight modification (Iida, Tomita, Idota, Takizawa, & Hayashi, 2006; Takizawa, Kitazato, Kishimoto, Tomita, & Hayashi, 2011). Male SD rats weighing 180–220 g were fasted for 12 h before the experiments. The surgery was performed according to previous reports (Kamei, Morishita, Ehara, & Takayama, 2008; Kamei, Morishita, & Takayama, 2009; Morishita, Kamei, Ehara, Isowa, & Takayama, 2007). Firstly, rats were anesthetized by intraperitoneal injection of sodium pentobarbital (100 mg/kg) and restrained in a supine position at 37 °C. Then, the ileum was exposed following a small midline incision carefully made in the abdomen, and ileum segments (approximately 10 cm) were selected by tying both ends of the segment for the in situ absorption experiment. Subsequently, the intestinal contents were washed out with 10 ml PBS warmed to 37 °C. The rats were left on the pad for an additional 30 min to recover from the elevated blood glucose concentration resulting from the surgery. After a period of rest, 1 ml CSO-DA-Ins NPs (50 IU/kg, 25 IU/kg) was redissolved separately in normal saline and injected into the ligated segments. CSO-Ins NPs (50 IU/kg, 25 IU/kg) groups were used as control groups. Blood samples were withdrawn from the caudal vein 5 min prior to dose administration, and 0.5, 1, 2, 3, 4, 5 and 6 h following administration. Blood glucose levels were measured by glucometer (ACCU-CHEK® Active Sensor, Roche Diagnostics, Mannheim, Germany).

2.7. Tissue histology

Histological studies were performed to evaluate the effect of NPs on the intestine. The method of evaluation of intestinal biopsies was as previously described (Whitehead, Shen, & Mitragotri, 2004). NPs redissolved in saline were administered by injecting into the intestinal loop and the animals were sacrificed after 1 and 4 h. The intestines exposed to NPs were excised, fixed in formalin, sectioned and stained using hematoxylin and eosin.

2.8. Statistical analysis

Statistical analysis for the determination of differences in the measured properties between groups was accomplished by one-way analysis of variance and determination of confidence intervals, performed using the Independent Samples *t*-test. All data are presented as mean values with standard deviations indicated (mean ± SD).

3. Result and discussion

3.1. Synthesis and characteristics of CSO-DA

In this study, CSO-DA was synthesized by a coupling reaction of DA and CSO. By controlling the amount of CSO, DA and EDC, CSO-DA copolymer with different substitution degrees (SD%) could be obtained. Fig. 1(A) shows the SD% of CSO-DA containing different amounts of DA determined by the TNBS method. TNBS is a substance that can react with the unreacted primary amino that are present on the CSO-DA molecules. The absorbance of the reaction production was measured by UV spectrophotometry. According to previous studies, the higher the SD% reached, the less amidogen was left and, consequently, the lower the surface charge density present. However, too high an SD% was disadvantageous for the stability of NPs and the interaction between the NPs and the intestinal mucosa. Based on the above, the SD% of CSO-DA used in this paper was determined to be 25.43%.

The ^{1}H NMR spectrum illustrated the binding between DA and CSO. As shown in Fig. 1(B), it can be seen that the peak at 1.9 ppm revealed the three N-acetyl protons of N-acetyl glucosamine and peak at 3 ppm showed the H2 proton of N-acetyl glucosamine or glucosamine residue. The ring protons of oligochitosan are considered to resonate at 3.4–3.8 ppm. The results are the same as the previous research (Layek & Singh, 2012). The new proton peaks of CH_3 (at 0.9 ppm) and CH_2 (at 1.1 ppm and 1.3 ppm) of DA were observed in the ^{1}H NMR spectrum of CSO-DA, while there no such peaks were observed in the same chemical shifts of the ^{1}H NMR spectrum of CSO.

Moreover, it is clear that the peaks of amide bands I and II of CSO are appeared at 1625 cm^{-1} and 1517 cm^{-1}, respectively (Fig. 1(C)). The new peaks of amide bands I and II were observed at 1632 cm^{-1} and 1526 cm^{-1} in the spectra of CSO-DA, respectively. The shifted peaks of amide bands I and II were caused by the amide band

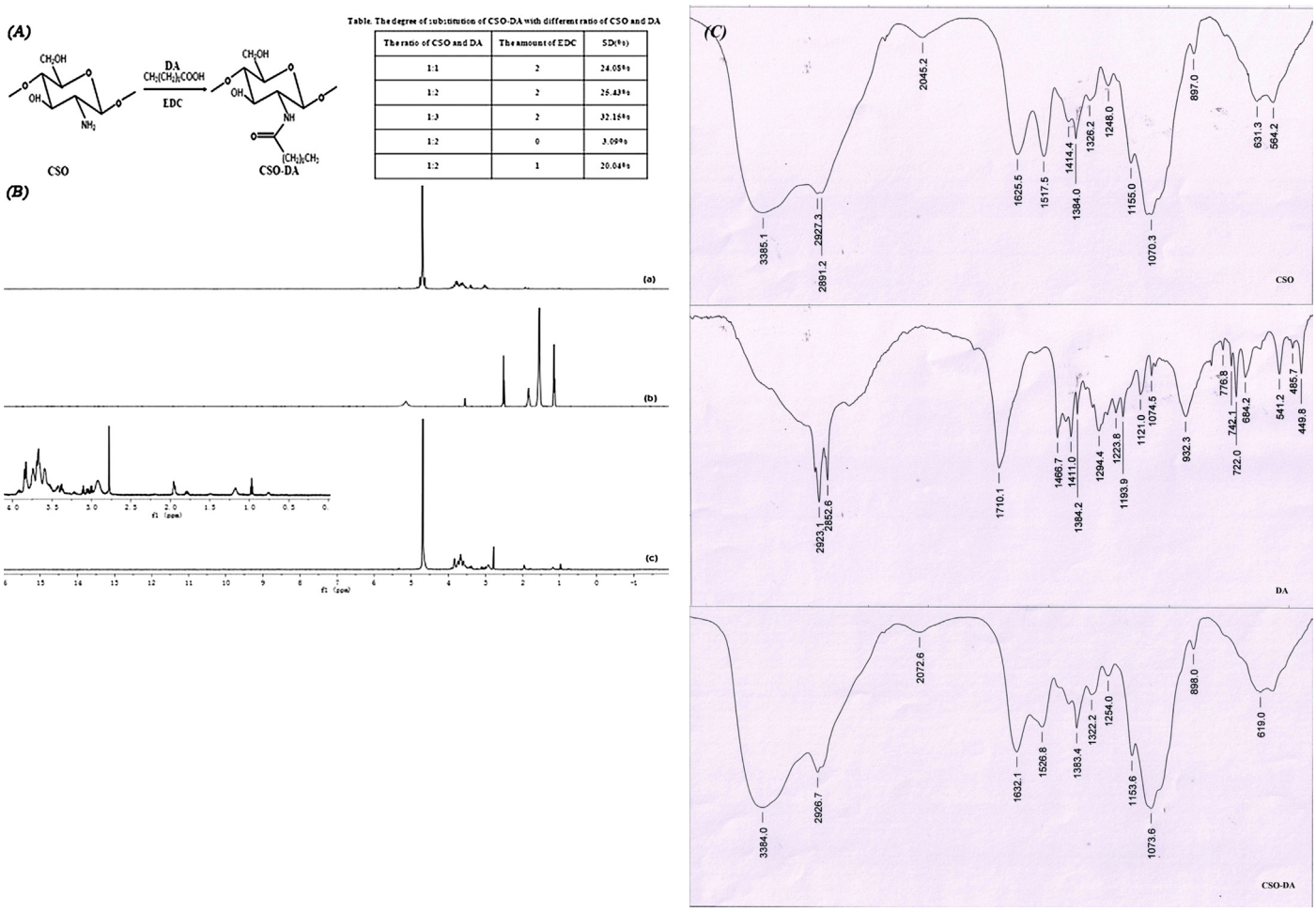

Fig. 1. (A) Synthetic route of CSO-DA conjugates and the SD of CSO-DA compounded with different amount of DA and EDC. (B) ^{1}H NMR spectra of CSO (a), DA (b) and CSO-DA (c). (C) FTIR spectra of CSO, DA and CSO-DA.

between CSO and DA. On the other hand, no absorption peak of the carboxyl groups of DA (1710 cm^{-1}) was found in the IR spectra of CSO-DA. These results demonstrated that CSO-DA was successfully synthesized by this method.

3.2. Preparation of nanoparticles and in vitro characterization

As reported by Berger (Berger, Reist, Mayer, Felt, & Gurny, 2004), chitosan can interact with negatively charged TPP forming inter- and intra-molecular cross-linkages, yielding ionically cross-linked nanoparticles. This method resulted in spontaneous formation of nanoparticles of smaller size with an opposite charge without using any organic solvent or surfacants, all of which help to maintain the biological activity of insulin. Since smaller particles are generally taken up more by intestinal epithelia than larger ones, the particle size served as a key factor in the formulation selection. The results of a preliminary investigation of the experimental conditions showed that nanoparticles could be obtained by varying the pH of CSO and the concentrations of TPP and CSO. CSO-NPs were prepared in the pH range of 2–8 and this was achieved by careful control of the acidity and alkalinity of the chitosan and TPP solutions, respectively. Three different systems could be identified visually: solution, suspension and aggregation. When the pH was ≤4 or ≥6, coacervation of the NPs would occur. As illustrated in Table 1, investigation focused on the pH from 4 to 6. Adjusting the pH of CSO to 5 or 5.5, suspensions were obtained and the optimal particle size was 189.0 ± 24.2 nm and 182.9 ± 79.6 nm, respectively. In respect of CSO-DA, this trend agreed well with previously results. Fixing the pH of CSO-DA at 5.5, and altering the ratio of CSO-DA and TPP, the nanoparticles formed stable colloidal particles with a narrow size distribution. This effect could be explained by the

Table 1
Average particle size of CSO NPs (a. Average particle size of CSO NPs obtained with varying pH and TPP/weight ratios of the nanoparticles) and CSO-DA NPs (b. Average particle size of CSO-DA NPs obtained with varying concentrations of CSO-DA and TPP of the nanoparticles (pH 5.5)).

Ratio (w/w)	pH = 4	pH = 5	pH = 5.5	pH = 6
(a)				
5:1	Aggregation	Weak opalescence	Weak opalescence	Aggregation
6.25:1	Aggregation	489.1 ± 62.4	234.4 ± 111.3	Aggregation
10:1	Aggregation	355.3 ± 44.9	216.7 ± 77.6	Aggregation
12.5:1	Aggregation	189.0 ± 24.2	182.9 ± 79.6	Aggregation

Concentration of CSO-DA (mg/ml)	Concentration of TPP (mg/ml)	Colloidal stability	Particle size
(b)			
0.5	1.0	Aggregation	–
1.0	0.5	Solution	191.1 ± 26.2
	0.8	Opalescence	175.3 ± 22.3
	1.0	Opalescence	296.5 ± 36.9
	1.2	Opalescence	361.4 ± 51.7
	1.5	Opalescence	594.2 ± 79.9
1.5	1.0	Opalescence	307.0 ± 36.2
2.0	1.0	Opalescence	479.9 ± 60.3
3.0	1.0	Opalescence	343.9 ± 37.2

nature of ionic gelation: ionotropic gelation occurred as the amino groups in CSO were protonated and charged positively. The degree of protonation of the amino groups in CSO increased as the acidity decreased (Makhlof et al., 2011). When the pH of CSO was adjusted to 5–5.5, more than 90% of the amino groups were protonated (Mao, Bakowsky, Jintapattanakit, & Kissel, 2006). On the other hand, TPP dissolved in water dissociated into hydroxide and tripolyphosphoric ions. At basic pH, both hydroxide and tripolyphosphoric ions could react ionically with the protonated amino groups of CSO by basic deprotonation and ionic cross-linking competitively. By making the pH acidic only $P_3O_{10}^{5-}$ ions existed and no additional anions were generated for deprotonation, so the particles formed would be only by ionic reaction (Dudhani & Kosaraju, 2010). Unexpectedly when the pH of TPP was 5–6, the particle distribution index (PDI) was too large and it did not conform to the pre-research by Dudhani. The reason for this might be that the intra-molecular binding of CSO chains with $P_3O_{10}^{5-}$ followed chain softening which was induced by OH^- ions (Kaloti & Bohidar, 2010). The amino sites on the CSO chain were partially bound to the hydroxyl ions preferentially so that the chain stiffness was reduced and, in the next step, tripolyphosphoric ions triggered intra-molecular linkages that folded the chains into nanoparticles. Considering all these factors in an integrated manner, in our study, the pH of CSO was set at 5.5 while the pH of TPP was unregulated.

The concentration was another key factor determining the particle size of NPs. Different formulations were prepared with different initial concentrations of CSO-DA (0.5–2.0 mg/ml) and TPP solutions (0.5–1.5 mg/ml). At very low or high concentrations either a clear solution was seen or large nanoparticles with a low colloidal stability were obtained. More specifically, on fixing the TPP concentration at 1 mg/ml, the particle size increased on increasing the concentration of CSO-DA. When the concentration of CSO-DA was set at 1 mg/ml, an increase in the TPP concentration led to a slight initial decrease in the nanoparticles followed by an enlargement after the TPP increased. When the TPP concentration was 0.8 mg/ml, a minimum of 175.3 ± 22.3 nm was obtained. As a TPP concentration less than 0.8 mg/ml, the nanoparticles were loose and inflated. On adding TPP, the intermolecular force increased and the particle size decreased. Once the TPP concentration was higher than the critical value, the nanoparticles aggregated easily. The particle size exhibited a slight increase following the addition of insulin, and it was only 200.6 ± 71.2 nm. Hence the final conditions were defined as a pH of 5.5, and concentrations of CSO-DA and TPP of 1.0 mg/ml and 0.8 mg/ml, respectively. The experimental results showed that the zeta potential was only 4.59 mV because the molecular weight of CSO was very low. It is known that the stability of insulin is poor in liquids. Thus, the nanoparticles obtained need be lyophilized to protect their biological activity. In order to avoid particle aggregation during the freeze-drying process, trehalose was used as a cryoprotectant. The concentration of trehalose was investigated and optimized as 1% (m/v) in a preliminary experiment. The size of freeze-dried NPs re-suspended in water was 209.9 ± 38.0 nm. TEM and SEM images of insulin loaded NPs prepared at pH 5.5 are shown in Fig. 2. The particle size was about 200 nm as illustrated. So, the result indicated that the loading of insulin in CSO-DA NPs was in agreement with the data measured by dynamic laser scattering.

An entrapment efficiency of 61.18% and a loading efficiency 5.56% were observed at pH 5.5, which were higher compared with other formations. The low loading efficiency of the insulin-loaded CSO-DA NPs may be due to weak intermolecular forces. It has been reported before that the pK_a of CSO was about 6.5, while the pI of insulin was about 5.5. The pH of the nanoparticle suspension obtained was approximately 6.0. In this case, the CSO was slightly positively charged, conversely, the insulin was slightly negative. The competitive interaction between the negative charge of insulin and the $P_3O_{10}^{5-}$ groups of TPP for protonated amino groups of CSO-DA resulted in low loading efficiencies.

3.3. In vitro release of insulin nanoparticles

A variety of techniques have been reported for the study of drug release from nanoparticles. The dialysis method has been frequently used for this purpose because it promotes the separation of the released drug from the drug in the carrier (Saarinen-Savolainen, Järvinen, Taipale, & Urtti, 1997). However, the drug is usually absorbed by the dialysis membrane and is hard to quantify. In addition, sink conditions are difficult to obtain inside the dialysis bag. All things considered, the release behavior was measured by ultracentrifugation.

Fig. 3 shows the in vitro release profile of insulin from nanoparticles which showed typical burst characteristics. In the first 0.5 h, the amount of insulin released from CSO NPs was as high as 66% at pH 1.2. In a release medium of pH 7.4, the amount of insulin released from CSO-DA NPs was only 49%, which was less than the CSO NPs value of 59%. The burst released insulin may account for the desorption of the protein close to the surface during the preparation of the NPs. After the first period, the rate of release fell as the predominant release mechanism changed to drug diffusion through the matrix (Papadimitriou, Bikiaris, Avgoustakis, Karavas, & Georgarakis, 2008). The remaining insulin in the nanoparticles was not completely released until the particles were completely eroded or had dissolved in release medium, which might be due to degradation and the interaction between the remaining insulin and the few free amino groups on the CSO segments (Zhang, Zhang, et al., 2008; Zhang, Teng, et al., 2008). The DA grafted NPs were released more slowly than the CSO NPs. This may have a protective effect on the insulin away from the GI environment. Moreover, it could be seen that the insulin was released more slowly in pH 7.4 PBS than at pH 1.2. A significant pH-dependence was apparent. One report has mentioned that pH-sensitive is also ion-sensitive (Berger et al., 2004). In acidic medium, both of the free ammonium groups on CSO-DA and insulin were charged positively. Their mutual repulsion and the entry of water together with counterions to neutralize these positive charges accelerated the release. However, when the pH was close to neutral, the CSO-DA was neutralized by TPP and insulin, so that the escape was slowed down. After 2 h, the release curve tended to be gentle. This may be explained by the swelling mechanism. The final cumulative release reached about 70%.

There was a problem that the release profile was almost the same between CSO-DA NPs and CSO NPs in acidic medium. There was no benefit in the drug going through the stomach without suffering any damage. It could be adjusted by bonding or combining with a polymer with special properties, such as HPMCP (Makhlof et al., 2011), and PMCP (Sajeesh & Sharma, 2006). The compound, methylcellulose phthalate (MCP), was first developed for use as a pharmaceutical excipient in enteric coating to protect pharmaceutical preparations from degradation caused by the low pH of gastric juices. The free carboxylic groups of MCP became negatively charged at higher pH values and acted as a driving force for the electrostatic interaction with CSO-DA. Furthermore, it was also able to protect the entrapped insulin against gastric degradation. Hence the CSO-DA/MCP NPs look like a promising idea to improve the CSO-DA NPs.

3.4. Bioactivity stability

The bioactivity stability profile of CSO-DA-Ins NPs and the insulin as control were investigated and the results are shown in Fig. 4. The blood glucose level of rats following subcutaneous administration of 5 IU/kg of nanoparticles was 26.15% of the initial

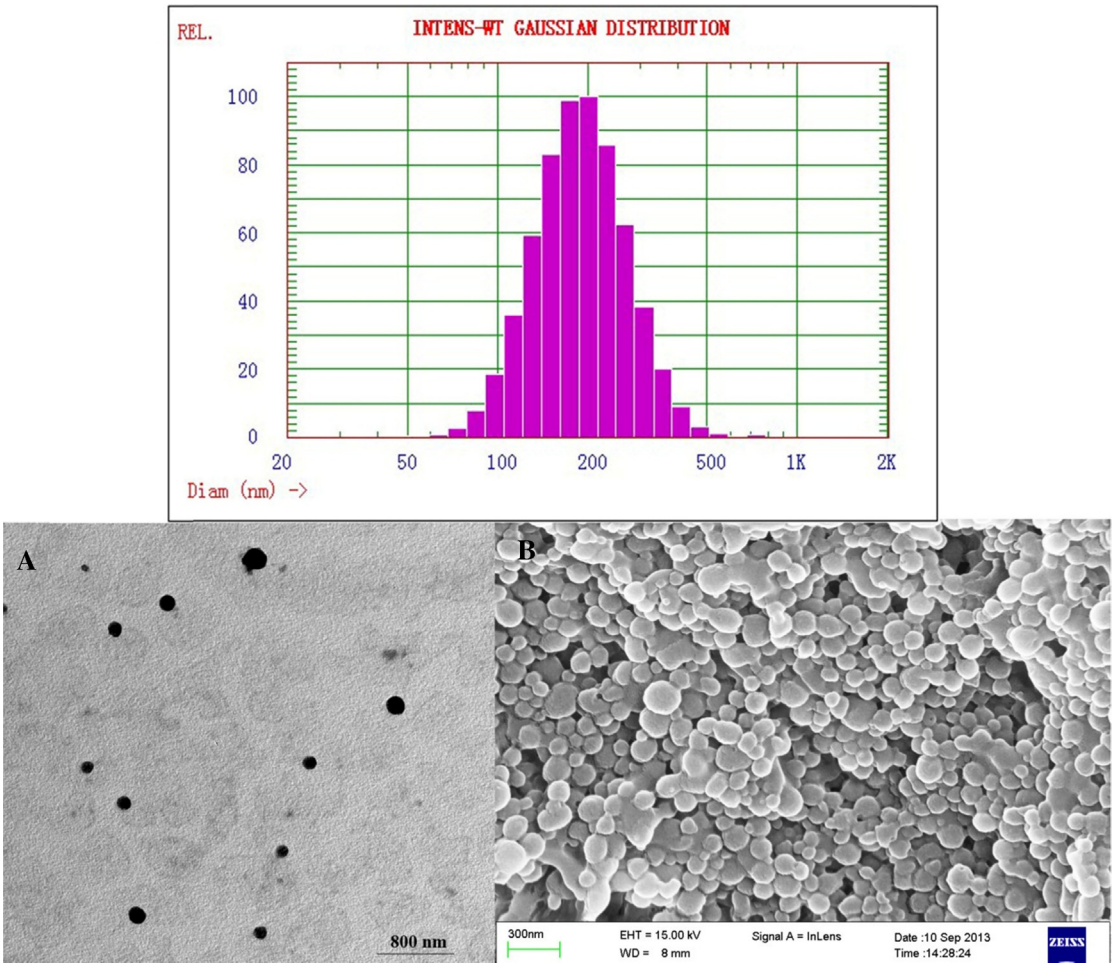

Fig. 2. TEM (A) and SEM (B) images with the particle size distribution of insulin loaded CSO-DA NPs.

level. A significant effect on reducing blood glucose was observed compared with the control, where 36.07% of the initial blood glucose level was obtained. Therefore, it was concluded that the bioactivity of insulin was well preserved after drug loading and lyophilizing.

3.5. Absorption experiments using the in situ loop method

Fig. 5 shows the variation in blood glucose of CSO-DA-Ins NPs and CSO-Ins NPs following in situ administration of insulin at 50 IU/kg and 25 IU/kg into ileal segments. It was found that both of the preparations exhibited a hypoglycemic effect. The blood glucose level began to come down from 30 min, and reached minimum at 1 h. The blood glucose level of CSO-DA NPs declined to 65.63% (25 IU/kg) lower than that of CSO NPs which declined to 83.18%

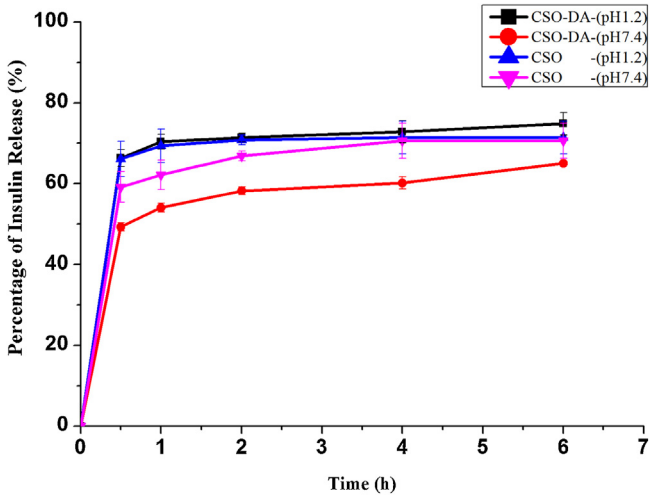

Fig. 3. (A) Insulin release profile from CSO-DA and CSO NPs in PBS of different pH value (pH = 1.2, 7.4) respectively by ultracentrifugation. (mean ± SD, $n = 3$).

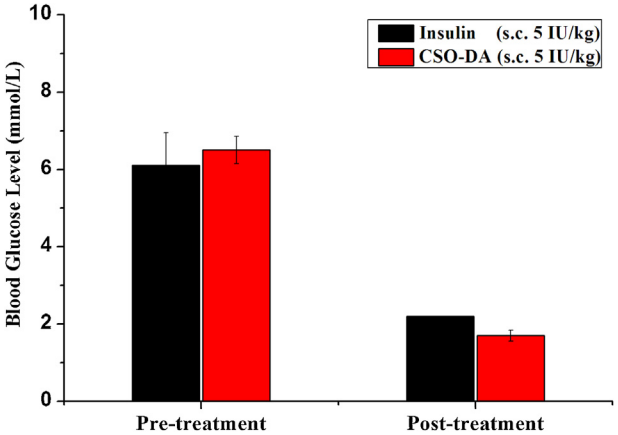

Fig. 4. The blood glucose level after injection of insulin released from CSO-DA NPs and insulin sample (5 IU/kg) at 1 h in rats ($n = 3$).

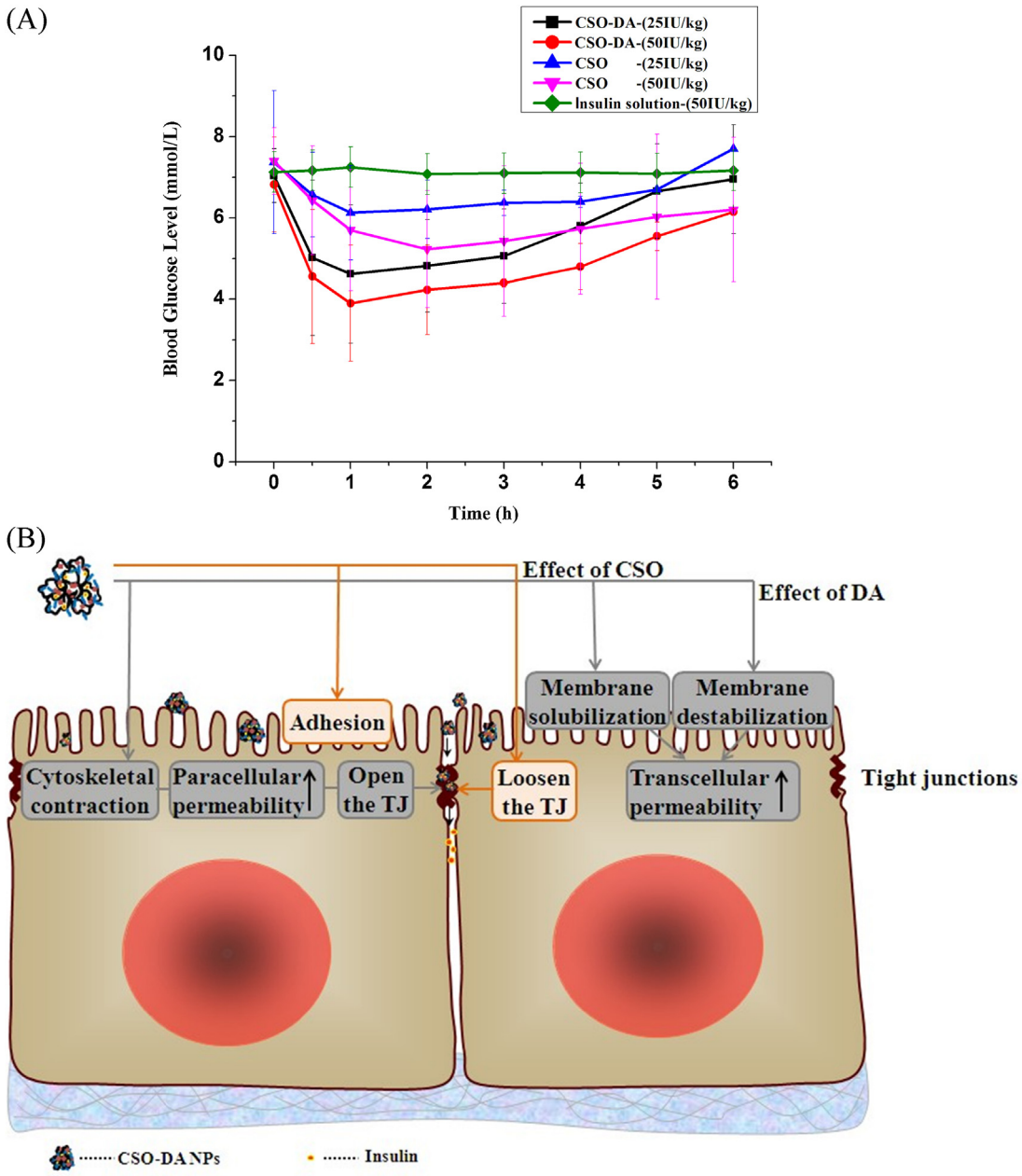

Fig. 5. (A) Hypoglycemic effect following ileal administration of insulin loaded CSO and CSO-DA NPs (25 IU/kg, 50 IU/kg). (B) Schematic illustrations of interaction between NPs and enterocyte.

(25 IU/kg). The reduction in blood glucose was greater in the animals receiving a higher dose of insulin (50 IU/kg). The degree of decline of CSO-DA 50 IU/kg was 57.18% which was better than that of CSO-DA 25 IU/kg. These results indicated that the reduction in the blood glucose levels depended on the insulin dose. As the nanoparticles could swell rapidly and promote drug absorption by intestinal administration rather than the oral route, the effect exhibited was marked and fast.

For orally administered drugs to be effective, they must be absorbed into the bloodstream. The mechanism behind this assumption was that the NPs shelled with CSO-DA may prolong their residence in the small intestine, infiltrate into the mucus layer, and subsequently produce transient opening of the tight junctions between epithelial cells. The insulin released from the broken-apart NPs could then permeate through the paracellular pathway into the bloodstream. It is known that tight junctions form a barrier to the uncontrolled absorption of noxious substances (gate function), and maintain epithelial polarity (fence function). Mucosal addition of sodium caprate could rapidly reduce the Caco-2 transepithelial electric resistance (TEER) by 40–65% ($T_{1/2}$, ~5 min) and, upon its removal, a marked recovery of TEER was observed (Chao et al., 1999). In addition, it has also been reported that the enhancement of mannitol and polyethylene glycol (PEG) 900 was more markedly increased in a dose-dependent manner. The results found in our work were analogous to those of previous researchers. The reason for this is at present unknown but might involve the environment in the intestinal lumen. The mild surfactant properties of DA also acted on destabilization and solubilization of enterocyte membranes, which impact on the contribution of the transcellular permeation pathway. On the other hand, the chitosan oligomers could provide adhesion to prolong the connection with the intestine and it has been reported that they can improve the intestinal absorption of insulin (Gao et al., 2008). Chitosan oligomers might loosen the tight junctions of the intestinal epithelium, thereby increasing the

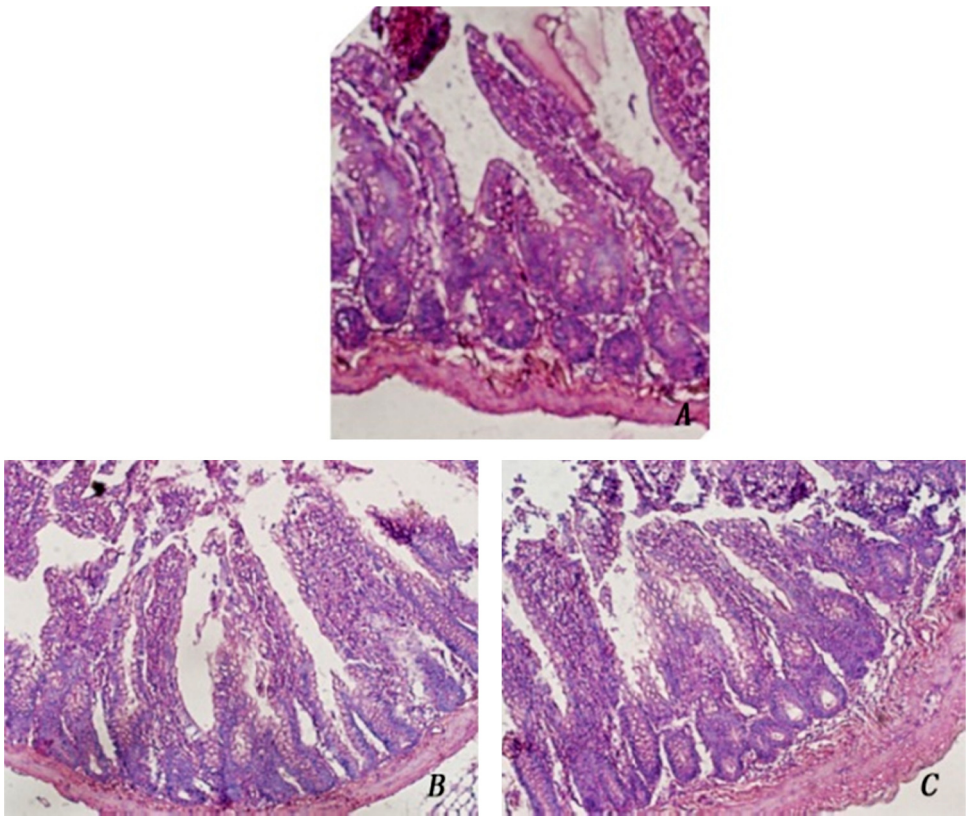

Fig. 6. Morphology of intestinal mucosa of rats after ileal administration of (A) physiological saline, (B) CSO-DA NPs after 1 h, and (C) CSO-DA NPs after 4 h.

permeability of drugs via the paracellular pathway. It was concluded that the binding and absorption enhancing effects of chitosan on epithelial cells were mediated through their positive charges and the interaction of chitosan with the cell membrane resulting in a structural reorganization of tight junction-associated proteins followed by enhanced transport through the paracellular pathway (Schipper, Olsson, Hoogstraate, Vårum, & Artursson, 1997). Furthermore, the absorption enhancing effect of chitosan oligomer for improving the intestinal absorption depended on its formation (Gao et al., 2008) and pH (Hsu et al., 2013). It may be connected with the deprotonation of chitosan by activation of integrin receptors on cell membranes. This is consistent with our experimental findings.

More experiments are needed to provide a better and complete explanation of how CSO-DA NPs enhance the intestinal absorption of insulin.

3.6. Tissue histology

Histological studies showed no evidence of significant changes in the structure of the intestine exposed to NPs compared with controls [Fig. 6a (control), b (1-h contact), c (4-h contact)]. There was no significant presence of inflammatory cells observed in samples. The villus structure was relatively normal and no disruption of the epithelium was observed. These results show that, at the doses used in this study, the CSO-DA delivery system did not produce any adverse effects on the intestine.

4. Conclusion

In this study, insulin loaded CSO-DA NPs were prepared by the ion-crosslinking method. The NPs had a suitable particle size distribution and exhibited pH-sensitive drug release in vitro. Results administration of redissolved NPs to rats indicated that the intestinal absorption of insulin was clearly improved compared with that of unmodified polymer NPs. Histopathology showed that the CSO-DA drug delivery system had a low toxicity with no mucosal damage. Therefore, the NPs developed in this study appear to be a promising delivery vehicle for the oral absorption of therapeutic proteins.

References

Aoki, Y., Morishita, M., & Takayama, K. (2005). Role of the mucous/glycocalyx layers in insulin permeation across the rat ileal membrane. *International Journal of Pharmaceutics*, *297*(1), 98–109.

Artursson, P., Lindmark, T., Davis, S. S., & Illum, L. (1994). Effect of chitosan on the permeability of monolayers of intestinal epithelial cells (Caco-2). *Pharmaceutical Research*, *11*(9), 1358–1361.

Asada, H., Douen, T., Waki, M., Adachi, S., Fujita, T., Yamamoto, A., et al. (1995). Absorption characteristics of chemically modified-insulin derivatives with various fatty acids in the small and large intestine. *Journal of Pharmaceutical Sciences*, *84*(6), 682–687.

Berger, J., Reist, M., Mayer, J. M., Felt, O., & Gurny, R. (2004). Structure and interactions in chitosan hydrogels formed by complexation or aggregation for biomedical applications. *European Journal of Pharmaceutics and Biopharmaceutics*, *57*(1), 35–52.

Bernkop-Schnürch, A., & Krajicek, M. E. (1998). Mucoadhesive polymers as platforms for peroral peptide delivery and absorption synthesis and evaluation of different chitosan–EDTA conjugates. *Journal of Controlled Release*, *50*(1), 215–223.

Calvo, P., Vila-Jato, J. L., & Alonso, M. J. (1997). Evaluation of cationic polymer-coated nanocapsules as ocular drug carriers. *International Journal of Pharmaceutics*, *153*(1), 41–50.

Chao, A. C., Nguyen, J. V., Broughall, M., Griffin, A., Fix, J. A., & Daddona, P. E. (1999). In vitro and in vivo evaluation of effects of sodium caprate on enteral peptide absorption and on mucosal morphology. *International Journal of Pharmaceutics*, *191*(1), 15–24.

Dudhani, A. R., & Kosaraju, S. L. (2010). Bioadhesive chitosan nanoparticles: Preparation and characterization. *Carbohydrate Polymers*, *81*(2), 243–251.

Fetih, G., Fausia, H., Okada, N., Fujita, T., Attia, M., & Yamamoto, A. (2006). Colon-specific delivery and enhanced colonic absorption of [Asu1, 7]-eel calcitonin using chitosan capsules containing various additives in rats. *Journal of Drug Targeting*, *14*(3), 165–172.

Gao, Y., He, L., Katsumi, H., Sakane, T., Fujita, T., & Yamamoto, A. (2008). Improvement of intestinal absorption of insulin and water-soluble macromolecular compounds by chitosan oligomers in rats. *International Journal of Pharmaceutics*, *359*(1–2), 70–78.

Gu, Y., Song, P., Li, T., & Sui, W. (2011). Synthesis and characterization of carboxymethyl-polyaminate chitosan and its adsorption behavior toward a reactive dye. *Carbohydrate Research*, *346*(6), 769–774.

Hsu, L. W., Ho, Y. C., Chuang, E. Y., Chen, C. T., Juang, J. H., Su, F. Y., et al. (2013). Effects of pH on molecular mechanisms of chitosan–integrin interactions and resulting tight-junction disruptions. *Biomaterials*, *34*(3), 784–793.

Hu, F. Q., Wu, X. L., Du, Y. Z., You, J., & Yuan, H. (2008). Cellular uptake and cytotoxicity of shell crosslinked stearic acid-grafted chitosan oligosaccharide micelles encapsulating doxorubicin. *European Journal of Pharmaceutics and Biopharmaceutics*, *69*(1), 117–125.

Iida, A., Tomita, M., Idota, Y., Takizawa, Y., & Hayashi, M. (2006). Improvement of intestinal absorption of P-glycoprotein substrate by D-tartaric acid. *Drug metabolism and Pharmacokinetics*, *21*(5), 424–428.

Illum, L. (1998). Chitosan and its use as a pharmaceutical excipient. *Pharmaceutical Research*, *15*(9), 1326–1331.

Imai, T., Shiraishi, S., Saitô, H., & Otagiri, M. (1991). Interaction of indomethacin with low molecular weight chitosan, and improvements of some pharmaceutical properties of indomethacin by low molecular weight chitosans. *International Journal of Pharmaceutics*, *67*(1), 11–20.

Kaloti, M., & Bohidar, H. B. (2010). Kinetics of coacervation transition versus nanoparticle formation in chitosan-sodium tripolyphosphate solutions. *Colloids and Surfaces B: Biointerfaces*, *81*(1), 165–173.

Kamei, N., Morishita, M., Ehara, J., & Takayama, K. (2008). Permeation characteristics of oligoarginine through intestinal epithelium and its usefulness for intestinal peptide drug delivery. *Journal of Controlled Release*, *131*(2), 94–99.

Kamei, N., Morishita, M., & Takayama, K. (2009). Importance of intermolecular interaction on the improvement of intestinal therapeutic peptide/protein absorption using cell-penetrating peptides. *Journal of Controlled Release*, *136*(3), 179–186.

Kim, K. Y., Kwon, S. L., Park, J. H., Chung, H., Jeong, S. Y., & Kwon, I. C. (2005). Physicochemical characterizations of self-assembled nanoparticles of glycol chitosan-deoxycholic acid conjugates. *Biomacromolecules*, *6*(2), 1154–1158.

Krug, S. M., Amasheh, M., Dittmann, I., Christoffel, I., Fromm, M., & Amasheh, S. (2013). Sodium caprate as an enhancer of macromolecule permeation across tricellular tight junctions of intestinal cells. *Biomaterials*, *34*(1), 275–282.

Kwon, S., Park, J. H., Chung, H., Kwon, I. C., Jeong, S. Y., & Kim, I. S. (2003). Physicochemical characteristics of self-assembled nanoparticles based on glycol chitosan bearing 5β-cholanic acid. *Langmuir*, *19*(24), 10188–10193.

Layek, B., & Singh, J. (2012). N-hexanoyl, N-octanoyl and N-decanoyl chitosans: Binding affinity, cell uptake, and transfection. *Carbohydrate Polymers*, *89*(2), 403–410.

Lehr, C. M., Bouwstra, J. A., Schacht, E. H., & Junginger, H. E. (1992). In vitro evaluation of mucoadhesive properties of chitosan and some other natural polymers. *International Journal of Pharmaceutics*, *78*(1), 43–48.

Makhlof, A., Tozuka, Y., & Takeuchi, H. (2011). Design and evaluation of novel pH-sensitive chitosan nanoparticles for oral insulin delivery. *European Journal of Pharmaceutical Sciences*, *42*(5), 445–451.

Makuška, R., & Gorochovceva, N. (2006). Regioselective grafting of poly (ethylene glycol) onto chitosan through C-6 position of glucosamine units. *Carbohydrate Polymers*, *64*(2), 319–327.

Mao, H. Q., Roy, K., Troung-Le, V. L., Janes, K. A., Lin, K. Y., Wang, Y., et al. (2001). Chitosan-DNA nanoparticles as gene carriers: Synthesis, characterization and transfection efficiency. *Journal of Controlled Release*, *70*(3), 399–421.

Mao, S., Bakowsky, U., Jintapattanakit, A., & Kissel, T. (2006). Self-assembled polyelectrolyte nanocomplexes between chitosan derivatives and insulin. *Journal of Pharmaceutical Sciences*, *95*(5), 1035–1048.

Miyazaki, S., Ishii, K., & Nadai, T. (1981). The use of chitin and chitosan as drug carriers. *Chemical & Pharmaceutical Bulletin*, *29*(10), 3067–3069.

Miyazaki, S., Yamaguchi, H., Yokouchi, C., Takada, M., & Hou, W. M. (1988). Sustained-release and intragastric-floating granules of indomethacin using chitosan in rabbits. *Chemical & Pharmaceutical Bulletin*, *36*(10), 4033–4038.

Morishita, M., Kamei, N., Ehara, J., Isowa, K., & Takayama, K. (2007). A novel approach using functional peptides for efficient intestinal absorption of insulin. *Journal of Controlled Release*, *118*(2), 177–184.

Muzzarelli, R. A. (1983). Chitin and its derivatives: New trends of applied research. *Carbohydrate Polymers*, *3*(1), 53–75.

Muzzarelli, R. A. (2010). Chitins and chitosans as immunoadjuvants and non-allergenic drug carriers. *Marine Drugs*, *8*(2), 292–312.

Muzzarelli, R. A., Boudrant, J., Meyer, D., Manno, N., DeMarchis, M., & Paoletti, M. G. (2012). Current views on fungal chitin/chitosan, human chitinases, food preservation, glucans, pectins and inulin: A tribute to Henri Braconnot, precursor of the carbohydrate polymers science, on the chitin bicentennial. *Carbohydrate Polymers*, *87*(2), 995–1012.

Nguyen, H. N., Wey, S. P., Juang, J. H., Sonaje, K., Ho, Y. C., Chuang, E. Y., et al. (2011). The glucose-lowering potential of exendin-4 orally delivered via a pH-sensitive nanoparticle vehicle and effects on subsequent insulin secretion in vivo. *Biomaterials*, *32*(10), 2673–2682.

Papadimitriou, S., Bikiaris, D., Avgoustakis, K., Karavas, E., & Georgarakis, M. (2008). Chitosan nanoparticles loaded with dorzolamide and pramipexole. *Carbohydrate Polymers*, *73*(1), 44–54.

Qiao, T., Wu, Y., Jin, J., Gao, W., Xie, Q., Wang, S., et al. (2011). Conjugation of catecholamines on magnetic nanoparticles coated with sulfonated chitosan. *Colloids and Surfaces A: Physicochemical and Engineering Aspects*, *380*(1), 169–174.

Saarinen-Savolainen, P., Järvinen, T., Taipale, H., & Urtti, A. (1997). Method for evaluating drug release from liposomes in sink conditions. *International Journal of Pharmaceutics*, *159*(1), 27–33.

Sajeesh, S., & Sharma, C. P. (2006). Cyclodextrin-insulin complex encapsulated polymethacrylic acid based nanoparticles for oral insulin delivery. *International Journal of Pharmaceutics*, *325*(1), 147–154.

Sawayanagi, Y., Nambu, N., & Nagai, T. (1982a). Directly compressed tablets containing chitin or chitosan in addition to mannitol. *Chemical & Pharmaceutical Bulletin*, *30*(11), 4216–4218.

Sawayanagi, Y., Nambu, N., & Nagai, T. (1982b). Use of chitosan for sustained-release preparations of water-soluble drugs. *Chemical & Pharmaceutical Bulletin*, *30*(11), 4213–4215.

Schipper, N. G., Olsson, S., Hoogstraate, J. A., Vårum, K. M., & Artursson, P. (1997). Chitosan as absorption enhancer for poorly absorbable drugs2: Mechanism of absorption enhancement. *Pharmaceutical Research*, *14*(7), 923–929.

Smith, S. G., Ravindranathan, S., Jayanthi, S., Suresh Kumar, T. K., & Zaharoff, D. A. (2014). Controlling chitosan-based encapsulation for protein and vaccine delivery. *Biomaterials*, *35*(14), 4382–4389.

Takayama, K., Hirata, M., Machida, Y., Masada, T., Sannan, T., & Nagai, T. (1990). Effect of interpolymer complex formation on bioadhesive property and drug release phenomenon of compressed tablet consisting of chitosan and sodium hyaluronate. *Chemical and Pharmaceutical Bulletin*, *38*(7), 1993–1997.

Takizawa, Y., Kitazato, T., Kishimoto, H., Tomita, M., & Hayashi, M. (2011). Effects of antioxidants on drug absorption in in vivo intestinal ischemia/reperfusion. *European Journal of Drug Metabolism and Pharmacokinetics*, *35*(3–4), 89–95.

Tozaki, H., Komoike, J., Tada, C., Maruyama, T., Terabe, A., Suzuki, T., et al. (1997). Chitosan capsules for colon-specific drug delivery improvement of insulin. *Journal of Pharmaceutical Sciences*, *86*(9), 1016–1021.

Whitehead, K., Shen, Z., & Mitragotri, S. (2004). Oral delivery of macromolecules using intestinal patches: Applications for insulin delivery. *Journal of Controlled Release*, *98*(1), 37–45.

Yoksan, R., Matsusaki, M., Akashi, M., & Chirachanchai, S. (2004). Controlled hydrophobic/hydrophilic chitosan: Colloidal phenomena and nanosphere formation. *Colloid & Polymer Science*, *282*(4), 337–342.

Zhang, X., Zhang, H., Wu, Z., Wang, Z., Niu, H., & Li, C. (2008). Nasal absorption enhancement of insulin using PEG-grafted chitosan nanoparticles. *European Journal of Pharmaceutics and Biopharmaceutics*, *68*(3), 526–534.

Zhang, X. G., Teng, D. Y., Wu, Z. M., Wang, X., Wang, Z., Yu, D. M., et al. (2008). PEG-grafted chitosan nanoparticles as an injectable carrier for sustained protein release. *Journal of Materials Science: Materials in Medicine*, *19*(12), 3525–3533.

Zhang, Y., Wu, X. R., Meng, L. K., Zhang, Y., Ai, R. T., Qi, N., et al. (2012). Thiolated Eudragit nanoparticles for oral insulin delivery: Preparation, characterization and in vivo evaluation. *International Journal of Pharmaceutics*, *436*, 341–350.

Zhao, M. D., Sun, Y. M., Fu, G. F., Du, Y. Z., Chen, F. Y., Yuan, H., et al. (2012). Gene therapy of endometriosis introduced by polymeric micelles with glycolipid-like structure. *Biomaterials*, *33*(2), 634–643.